Inorganic Chemistry

ARTICLE

pubs.acs.org/IC

Reaction Mechanism of the Reverse Water−Gas Shift Reaction Using First-Row Middle Transition Metal Catalysts L′M (M = Fe, Mn, Co): A Computational Study

Cong Liu, Thomas R. Cundari,* and Angela K. Wilson*

Department of Chemistry and Center for Advanced Scientific Computing and Modeling (CASCaM), University of North Texas, Denton, Texas 76203-5070, United States

Supporting Information

ABSTRACT: The mechanism of the reverse water−gas shift reaction ($CO_2 + H_2 \rightarrow CO + H_2O$) was investigated using the 3d transition metal complexes L′M (M = Fe, Mn, and Co, L′ = parent β-diketiminate). The thermodynamics and reaction barriers of the elementary reaction pathways were studied with the B3LYP density functional and two different basis sets: 6-311+G(d) and aug-cc-pVTZ. Plausible reactants, intermediates, transition states, and products were modeled, with different conformers and multiplicities for each identified. Different reaction pathways and side reactions were also considered. Reaction Gibbs free energies and activation energies for all steps were determined for each transition metal. Calculations indicate that the most desirable mechanism involves mostly monometallic complexes. Among the three catalysts modeled, the Mn complex shows the most favorable catalytic properties. Considering the individual reaction barriers, the Fe complex shows the lowest barrier for activation of CO_2.

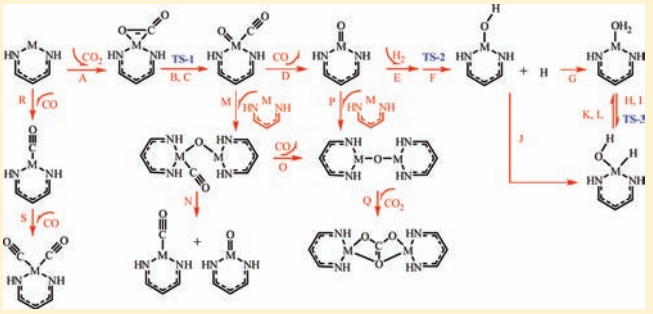

INTRODUCTION

Carbon dioxide interacting with transition metals has been the focus of research in many fields, including catalytic reduction of CO_2, metal corrosion, CO_2 capture, and CO_2 fixation.[1−12] Recent experimental and computational studies have focused on CO_2 reacting with metal/metal oxide surfaces,[8,13−16] metal−organic frameworks,[17−20] and transition metal complexes[2,9−12,21] because of their significance to greater utilization and sequestration of this greenhouse gas.

The thermodynamic stability of carbon dioxide provides a major challenge in converting CO_2 to more useful products. Its reactions often require high temperatures and/or high pressures.[22,23] Thus, activation of CO_2 by catalytic means is extremely important. Transition metal complexes have shown the ability to activate the C═O bond of CO_2. First-row transition metals have become a great focus of interest.[2,9−12,21] Some have been chosen by nature to activate CO_2; reduction of CO_2 to CO can be mediated by enzymes such as nitrogenase (e.g., MoFeP and FeP) and carbon monoxide dehydrogenase.[10] Other first-row transition metal complexes have been studied as well, especially middle to late series.[11,12,21,24] For example, Lu et al.[21] studied Fe(I)-mediated reductive cleavage and coupling of CO_2; the tris(phosphino)borate complex [$PhBP^{CH2Cy3}$] of Fe reacts readily with CO_2 at ambient temperature to generate two products with a Fe(μ-CO)(μ-O)Fe core and a Fe(μ-η^2:η^2-oxalato)Fe core. Isaacs et al.[11] reported the electrocatalytic reduction of CO_2 using aza-macrocyclic complexes of Ni(II), Co(II), and Cu(II). The electronic spectra indicate that the electrochemical reduction of CO_2 is due to the presence of a formal 1+ metal, although the presence of the reduced ligand is also essential. Li et al.[12] reported DFT (density functional theory) studies on coupling reactions of CO_2 with alkynes using Ni(0) complexes, Ni(DBU)$_2$(HC≡CX) (DBU = diazabicycloundecene, X = Me, OMe, or CN). Calculations show that an associative mechanism is preferred in the coupling reactions. Of three model terminal alkynes, X = OMe gives the lowest barrier (17.1 kcal/mol).

In addition to interest in varying transition metal centers, research has shown that some ligands also have a significant impact upon the bonding and activation of small molecules and complexes. For example, β-diketiminate ligands have received increased attention because of their ability to stabilize low coordinate transition metal centers,[26] which contributes to activation of small molecules.[27−44] Smith et al.[27] studied the interaction of N_2 and iron(I) complexes [L^RFeCl]$_n$ and [L^RFeH]$_{in}$ (L^R = β-diketiminate, R = Me, ^{t}Bu). In the product, L^RFeNNFeL^R, the N−N bond is substantially weakened, and calculations (DFT and multiconfiguration self-consistent field) indicate that the bond weakening arises from back-bonding into the N_2 π^* orbitals. Similarly, Ding et al.[29] synthesized dicobalt(I)−N_2 complexes L^RCoNNCoL^R and also observed N−N weakening. Pfirrmann et al.[30] investigated N_2 and H_2 activation using

Received: March 23, 2011
Published: August 12, 2011

Scheme 1. Proposed Reaction Pathways and Side Reactions for RWGS Reaction Catalysis

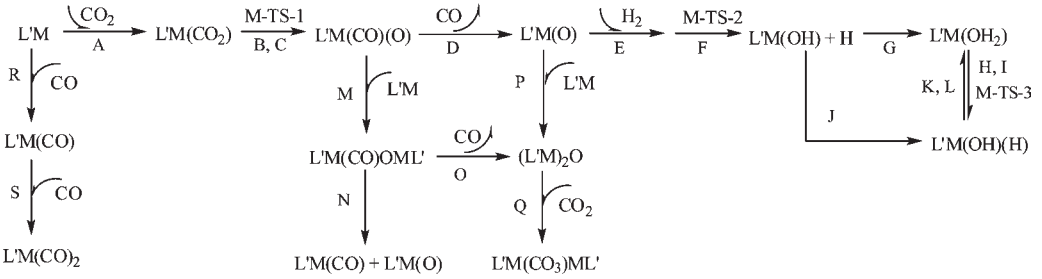

Ni β-diketiminate complexes, $[L^{Me}Ni]_2$ and $L^{Me}Ni(\mu\text{-Br})Li(thf)_2]_2$. The XRD (X-ray diffraction) results show that reaction with H_2 generates $L^{Me}Ni(\mu\text{-H})_2$, while N_2 inserts into the Ni—Ni bond to form $[(L^{Me}Ni)_2(N_2)]$. Pierpont and Cundari[31] investigated methane C—H bond activation by $L_nM{=}E$ (L_n = β-diketiminate, dihydrophosphinoethane (dhpe); M = Fe, Ni, Co; E = NCF_3, NCH_3, O) using hybrid DFT (B3LYP) calculations. Activation of methane via $L_nM{=}E$ is both thermodynamically and kinetically feasible, and lower overall reaction Gibbs free energies were found with the proximity of fluorinated substitutes to the metal center, with the β-diketiminate ligands exhibiting the greatest sensitivity to substituent effects. One recent study by Sadique et al.[32] described reduction of CO_2 to CO and carbonate using a low-coordinate iron—dinitrogen complex, $L^{tBu}FeNNFeL^{tBu}$ (where L^{tBu} = 2,2,6,6-tetramethyl-3,5-bis[(2,6-diisopropylphenyl)imino]hept-4-yl), by forming a four-coordinate iron dicarbonyl complex, $L^{tBu}Fe(CO)_2$, and a bridging carbonate complex, $L^{tBu}Fe(\mu\text{-}OCO_2)FeL^{tBu}$. Recently, Ariafard et al. reported a very interesting DFT study of the mechanism of the reductive cleavage of CO_2 by $L^{Me}FeNNFeL^{Me}$; CO_2 inserts between two Fe atoms of $L^{Me}FeNNFeL^{Me}$, then N_2 is released, followed by cleavage of CO_2 and formation of an $L^{Me}Fe{-}O{-}Fe(CO)\ L^{Me}$ structure. The overall reductive cleavage reaction was predicted to be exergonic by 120 kJ/mol.[42] $L^{Me}Fe{-}O{-}Fe(CO)L^{Me}$ then releases CO to form $L^{Me}Fe{-}O{-}FeL^{Me}$, which can readily react with CO_2 to give $L^{Me}Fe{-}O{-}Fe(CO)\ L^{Me}$.[42]

Recently, we reported a modeling study of the thermodynamics of the component reactions of a RWGS (reverse water—gas shift) catalyst ($CO_2 + H_2 \rightarrow CO + H_2O$) using β-diketiminate complexes L′M of all 3d metals (L′ = β-diketiminate; M = Sc, Ti, V, Cr, Mn, Fe, Co, Ni, Cu, and Zn).[1] B3LYP calculations showed that the β-diketiminate metal catalyst models were thermodynamically viable for coordination of CO_2. These metals generally displayed two linkage isomers for the binding of CO_2: η^2(C,O) and η^2(O), between which η^2(C,O) is predominant for the first eight metals from Sc to Ni. In general, metals from the middle of the 3d series, Mn and Fe catalyst models, displayed more favorable thermodynamics for the component reactions for the RWGS reaction than the other metals, arising from a balance between more favorable CO_2 activation by early 3d metals and more favorable reduction reactions by late 3d metals.

On the basis of the aforementioned thermodynamic results, it is interesting to investigate the reaction barriers of these reactions for the metals that display the most promising thermodynamics. Therefore, in this paper, possible reaction pathways are assessed for the RWGS reaction catalysis. The research is focused on β-diketiminate complexes of Fe, Mn, and Co. Under experimental conditions side reactions need to be considered, for example, ligand degradation; however, in this study, we focus on intrinsic CO_2 chemistry with different late 3d metal centers. The proposed reaction pathways are shown in Scheme 1 and are inspired by recent experimental reports from the Peters[21] and Holland[27−29,32,33,44] groups. The first reaction (step A) occurs between L′M and CO_2 and forms a L′M(CO_2) complex, which then goes through a TS (transition state) for C═O activation to form L′M(CO)(O) (steps B and C). Subsequently, L′M(CO)(O) may release CO and form L′M(O) (step D) or react with L′M and form a bimetallic complex L′M(CO)OML′ (step M). In step D, the oxo complex L′M(O) may react with another L′M to give a μ-oxo complex $(L'M)_2O$ (step P) or react with H_2 and form a L′M(OH) and H radical (steps E and F). The species L′M(OH) and H mixture may form either an aqua complex L′M(OH_2) (step G) or a hydroxyl/hydride L′M(OH)(H). The latter may then form L′M(OH_2) via a hydrogen migration TS (steps H, I, K, and L). The final product of the hydrogenation, L′M(OH_2) versus L′M(OH)(H), depends on the thermodynamic stability of these two complexes. It is notable that L′M(OH_2) will release H_2O and yield back the model catalyst; however, L′M(OH)(H) may also react with CO_2.[12] On the other hand, L′M(CO)OML′ may split into L′M(CO) and L′M(O) or release CO to form $(L'M)_2O$, which may react with another CO_2 and generate a bridging carbonate complex L′M(CO_3)ML′. Since CO is one of the products in the RWGS reaction, it may conceivably ligate metal centers. The complex L′M(CO) may ligate another CO molecule and form a dicarbonyl complex L′M($CO)_2$. The detailed reaction in Scheme 1 provides insight as to the feasibility of the RWGS catalysis, including reaction barriers and side reactions. Combined with our previous research, we are able to describe reaction mechanisms and compare the favorability of the various pathways for Fe, Mn, and Co catalyst models.

COMPUTATIONAL METHODS

The Gaussian09[45] program was used to fully optimize all of the structures reported in this paper using DFT methods. Geometry optimizations and frequency calculations were carried out using the B3LYP functional.[46] Reaction barriers were also calculated using the B-97D functional,[47] and results showed good agreement (within a few kcal/mol) with B3LYP results. However, B-97D geometry optimizations of complexes in this paper took much longer than B3LYP optimizations; therefore, in the present research only B3LYP results are reported. Frequency calculations were performed to identify all of the stationary points as minima or transition states and to provide Gibbs free energies at 298.15 K and 1 bar in the gas phase. The 6-311+G(d) basis set was used for initially identifying all pertinent minima, and then the larger aug-cc-pVTZ basis set was used for further optimizing all found stationary points and obtaining the vibrational frequencies (unscaled) needed for the free energy calculations at STP. These two basis sets gave

dx.doi.org/10.1021/ic200602v |*Inorg. Chem.* 2011, 50, 8782–8789

very similar results on reaction Gibbs free energies and reaction barriers (see Supporting Information). The maximum differences in reaction Gibbs free energies are 3.7 kcal/mol for Fe complexes, 3.9 kcal/mol for Mn complexes, and 2.1 kcal/mol for Co complexes.

Solvent effects were calculated for the reaction barriers using two *n*-pentane ($\varepsilon = 1.8371$) and diethyl ether ($\varepsilon = 4.2400$) and the polarizable continuum modeling (PCM) solvent model in Gaussian 09.[45] The results indicate that continuum solvent effects do not have a significant contribution to free energies (See Supporting Information).

The metals in the L′M catalyst models have a 1+ formal oxidation state to best coincide with complexes reported by Holland and coworkers.[28] All reasonable conformations and possible multiplicities of the complexes are taken into account.

RESULTS AND DISCUSSION

a. Geometries and Ground State Multiplicities. The pathways and side reactions considered are summarized in Scheme 1. Scheme 2 shows the optimized structures of all Fe complexes studied using the B3LYP/aug-cc-pVTZ level of theory; L′Fe, L′Fe(CO), L′Fe(O), L′Fe(CO_2), and L′Fe(OH_2) have been discussed in our previous report.[1] The structures of Mn and Co complexes show strong similarity with Fe complexes (Schemes S1 and S2, Supporting Information); thus, for the sake of brevity, only the Fe complexes are shown in Schemes 1 and 2. Taking Fe complexes as an example, for steps A−F, Scheme 1, the reactions go through two transition states, **Fe-TS-1** and **Fe-TS-2** (Scheme 2). The imaginary mode of **Fe-TS-1**, C═O oxidative addition, was found to entail vibration between C4 and O2 (C4 and O2 move away from each other), indicating formation of intermediate L′Fe(CO)(O). In **Fe-TS-2**, which connects L′Fe(O) and the system of L′Fe(OH) and H, the vibration in the imaginary mode occurs between the two hydrogen atoms, H6 and H7, in which H6 tends to bond O1 (coordinated to Fe) while H7 is moving to the Fe atom. This leads to generation of L′Fe(OH) and an H radical, which may then plausibly form either L′Fe(OH_2) or L′Fe(OH)(O) if the H atom adds to the oxygen or metal, respectively. Another transition state, **Fe-TS-3**, connecting L′Fe(OH_2) and L′Fe(OH)(H) involves vibration of atoms H7 and O1 (Scheme 2).

In addition to monometallic intermediates, some bimetallic complexes may also participate in the catalysis. L′Fe(CO)OFeL′ may be formed from the reaction of L′Fe(CO)(O) and L′Fe. The calculations show that during this reaction the Fe atom of L′Fe is more likely to bond with O1 in L′Fe(CO)(O) instead of C7 or O2 in L′Fe(CO)(O) (Scheme 2). Then, L′Fe(CO)OFeL′ is possibly split into L′Fe(O) and L′Fe(CO) or may release a CO and form $(L'Fe)_2O$. The latter may also form from reaction of L′Fe(O) and L′Fe. The complex $(L'Fe)_2O$ formally has two lone pairs on O1 and could attract another CO_2 molecule and form a carbonate bridge molecule L′Fe(CO_3)FeL′ in which Fe2 bonds to O2 and O3 while Fe1 only bonds to O1; the two β-diketiminate ligands are in different planes. The bridging carbonate is one of two products isolated by Holland et al.[32] in the reaction of $L^{R}FeNNFeL^{R}$ with CO_2.

The calculated structures of $(L'Fe)_2O$, L′Fe(CO_3)FeL′, and L′Fe$(CO)_2$ are in good agreement with some bulkier β-diketiminate derivatives experimentally characterized by the Holland group.[32,44] The corresponding bond lengths and bond angles from calculations and experiments are organized in Table S1 (Supporting Information). For instance, $(L'Fe)_2O$ shows similar structure with $(L^{tBu}Fe)_2O$ that can be synthesized from $(L^{tBu}FeH)_2$ or $(L^{tBu}FeN)_2$.[44] It has been reported that $(L^{tBu}Fe)_2O$ reacts with CO_2 rapidly at room temperature to generate a carbonate−diiron complex $L^{tBu}Fe(CO_3)FeL^{tBu}$, which illustrates step Q in Scheme 1. The calculated structure of L′Fe(CO_3)FeL′ is in good agreement with the crystal structure of $L^{tBu}Fe(CO_3)FeL^{tBu}$.[32]

Scheme 2. Optimized Structures of Fe Complexes (B3LYP/aug-cc-pVTZ)[48]

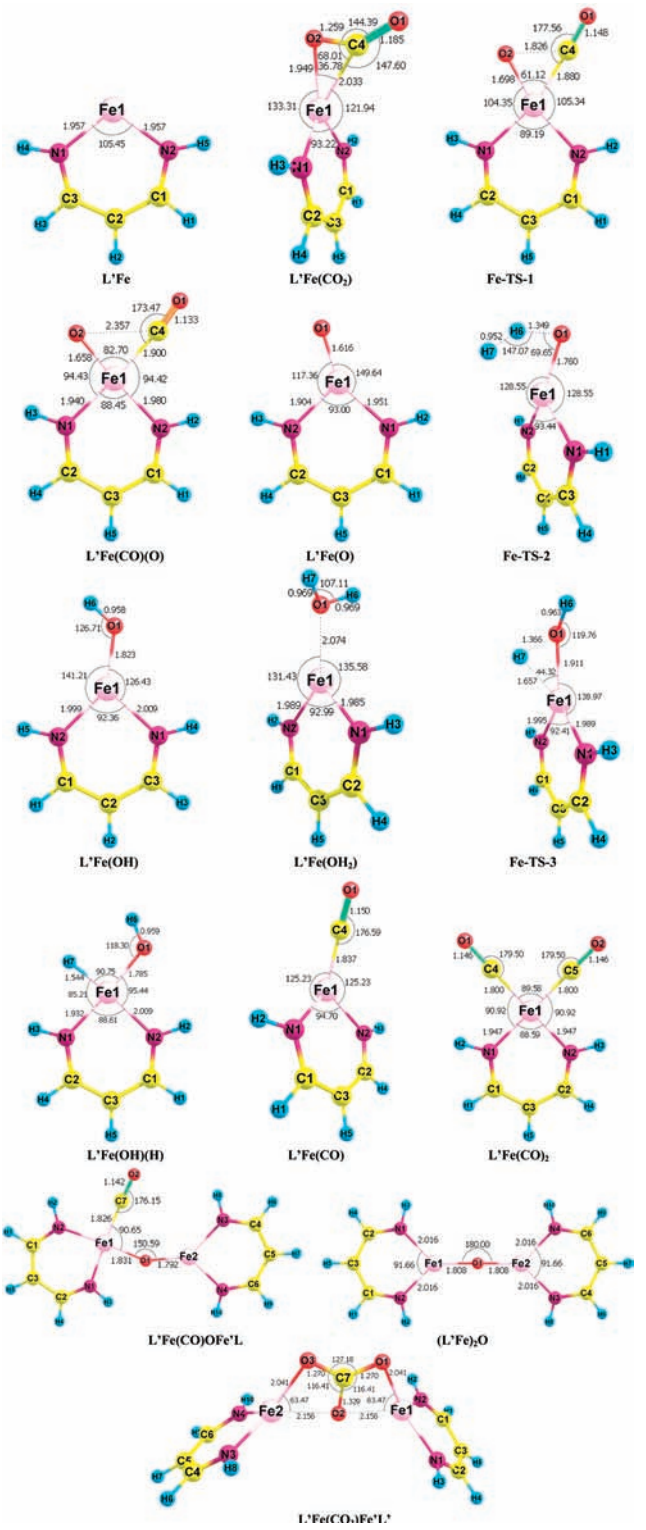

dx.doi.org/10.1021/ic200602v |*Inorg. Chem.* 2011, 50, 8782–8789

Table 1. Ground State Multiplicity of All Complexes

metal	L′M	L′M(CO_2)	M-TS-1	L′M(CO)(O)	L′M(O)
Fe	4	4	4	4	4
Mn	7	5	3	3	5
Co	3	3	3	3	5
metal	M-TS-2	L′M(OH)	L′M(OH_2)	M-TS-3	L′M(OH)(H)
Fe	6	5	4	4	4
Mn	5	6	7	7	5
Co	5	4	3	3	3
metal	L′M(CO)	L′M(CO_2)	L′M(CO)OML′	(L′M)$_2$O	L′M(CO_3)ML′
Fe	4	2	3	9	9
Mn	5		11	11	11
Co	3		5	7	7

Moreover, L′Fe($CO)_2$ was found to have a similar geometry to the crystal structure of L$^{t\mathrm{Bu}}$Fe($CO)_2$, in which the C−Fe−C angle (81.44°) is smaller than that in L′Fe($CO)_2$ (89.58°), perhaps due to the steric effect of the bulky *t*Bu ligands.[32]

Mn and Co complexes show very similar structural behaviors with Fe complexes (Scheme S1 and S2, Supporting Information). One exception for Mn complexes is L′Mn(CO)(O), which has a tetrahedral coordination geometry about the Mn while the Fe complex has a planar structure. For Co complexes, one exception is the transition state **Co-TS-2**: the position of H7 is quite far away (Co−H7 bond length is 2.86 Å) from the Co atom and thus quite different from **Fe-TS-2** and **Mn-TS-2**, in which the vibrations of H7 show that H7 tends to move toward the metal center while increasing its distance from H6 (Scheme S1, Supporting Information). Also, the Mulliken atomic spin densities in L′Co(OH) show that the spin density at the Co atom (2.46 e^-) is significantly lower than those of Fe and Mn (Mn 4.72 e^-, Fe 3.65 e^-), which implies that in **Co-TS-2** O1 has a greater propensity to react with H7 from a spin-coupling perspective and form L′Co(OH_2), compared with the O1 atoms in **Fe-TS-2** and **Mn-TS-2**. However, the stability of the two tautomers, L′Co(OH_2) and L′Co(OH)(H), depends on the thermodynamic calculations.

b. Ground State Multiplicity and Spin-State Crossing. All feasible multiplicities for all of the complexes are considered in the present calculations (Table 1). Generally, most mono-Fe complexes maintain a multiplicity of 4. The bis-carbonyl complex, L′Fe($CO)_2$, shows a lower multiplicity of 2, which is reasonable due to coordination of the strong field ligand CO. L′Fe(CO_3)Fe′L has a multiplicity of 9, indicating weak interaction between the two metal centers mediated by the bridging CO_3^{2-} group. The calculated Mulliken spin densities of L′Fe(OH) (Fe, 3.65 e^-; O, 0.22 e^-) suggest that L′Fe(OH)(O) is more likely to form based on the Fe being a more "radical" center. However, the final structure significantly depends on the thermodynamics; BDE(O−H) is expected to be much stronger than BDE(Fe−H). For Mn complexes, three transition states **Mn-TS-1**, **Mn-TS-2**, and **Mn-TS-3** were found to have similar imaginary frequencies as compared with the corresponding Fe transition states. Most Co complexes maintain a consistent triplet state. Since the spin states of the intermediates/transition states play an important role in the energetic landscape, we discuss below several examples of spin state crossing.

Scheme 3. Reaction Coordinate and Relative Energies of Involved Spin States (B3LYP/6-311+G(d))

(a). Hydrogenation of L'Fe(O)

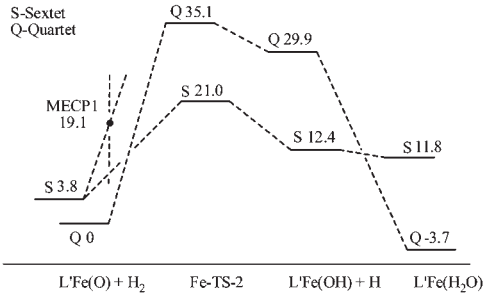

(b). Dissociation of CO from L'Fe(CO)OFeL'

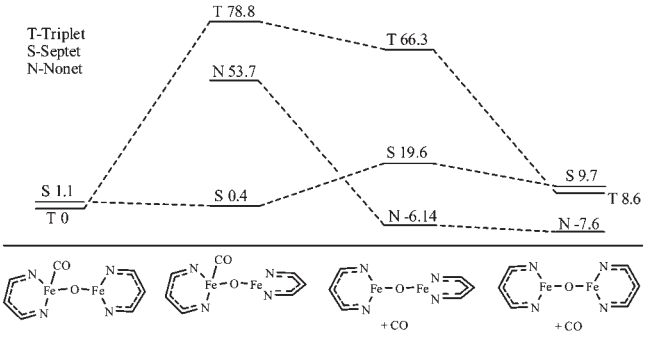

(c). Dissociation of Co from L'Mn(CO_2)

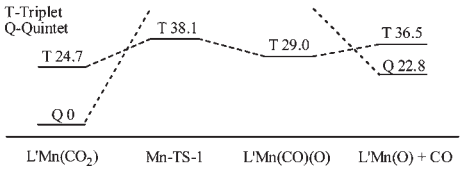

Hydrogenation of L′Fe(O) involves two spin states, a quartet and sextet (Scheme 3a). The ground state of L′Fe(O) is a quartet, while the sextet is 3.8 kcal/mol higher. The calculations indicate that there is a spin-state crossover on the way to the transition state Fe-TS-2 and another spin crossover leading to a quartet product, L′Fe(H_2O). A minimum energy crossing point (MECP) was indentified using the partial optimization method;[49,50] MECP1 lies 19.1 kcal/mol above quartet-L′Fe(O) + H_2. L′Fe(OH) has a lower multiplicity (Table 1) than L′Fe(O) (step F). Thus, the lowest energy pathway of reaction involves crossing from an initial quartet state L′Fe(O) to a sextet transition state and eventually back to a quartet L′Fe(H_2O).

Another interesting spin-crossing reaction is dissociation of CO from L′Fe(CO)OFeL′(Scheme 3b). Three spin states participate in the reaction: triplet, septet, and nonet. Calculations found that the ground state of L′Fe(CO)OFeL′ is a triplet state, which has coplanar L′ rings (we call it S-L′Fe(CO)OFeL′, "S" stands "same plane"), while a septet ground state for L′Fe(CO)OFeL′ with the two L′ rings perpendicular to each other only is 0.4 kcal/mol higher energy than S-L′Fe(CO)OFeL′ (termed P-L′Fe(CO)OFeL′, "P" stands for "perpendicular"). The tiny energy difference suggests that the rotation of L′ rings around the Fe−O−Fe axis should be facile and the spin-state

dx.doi.org/10.1021/ic200602v |*Inorg. Chem.* 2011, 50, 8782–8789

Scheme 4. Reaction Gibbs Free Energy Diagram for Fe Complexes Reactions (B3LYP/aug-cc-pVTZ)

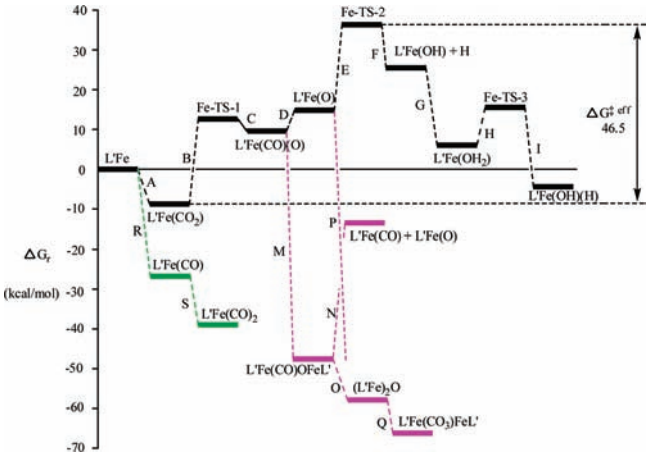

crossing from triplet S-L′Fe(CO)OFeL′ to septet P-L′Fe(CO)OFeL′ should also be quite feasible. Interestingly, calculations predict that $(L'Fe)_2O$ keeps a nonet ground state, whether or not the L′ rings are in the same plane. Thus, the proposed reaction coordinate is that L′Fe(CO)OFeL′ starts with a triplet S structure, undergoes a quick internal rotation to cross to a septet P structure, and then experiences another intersystem crossing from septet to nonet, yielding P-$(L'Fe)_2O$ + CO and finally giving S-$(L'Fe)_2O$ + CO. The spin-state crossover from the septet P-L′Fe(CO)OFeL′ to the nonet P-$(L'Fe)_2O$ agrees with the report of Ariafard et al.[42] It is notable that in their report they found the ground state of $L^{Me}Fe(CO)OFeL^{Me}$ to be a septet P structure instead of a triplet S structure. This is possible because the methyl groups on the ligands could generate a steric effect to favor the perpendicular structure. Similar structural phenomena were observed for $(L^{Me}Fe)_2O$.

Reactions of Mn complexes also involve multiple spin states. An example is the dissociation of CO from L′Mn(CO_2) (Scheme 3c). The ground state triplet L′Mn(CO_2) was found to have a much lower energy (24.7 kcal/mol) than the quintet. However, the calculations did not locate either the triplet transition state Mn-TS-1 or the triplet intermediate L′Mn(CO)(O). Optimization of the triplet Mn-TS-1 and L′Mn(CO)(O) always result in L′Mn(CO_2). We suggest that the triplet Mn-TS-1 and L′Mn(CO)(O) probably have very high energy. Therefore, the lowest energetic pathway involves a triplet L′Mn(CO_2) undergoing a quintet transition state Mn-TS-1 and a quintet intermediate L′Mn(CO)(O) and finally giving triplet L′Mn(O) + CO.

c. Reaction Gibbs Free Energies and Reaction Barriers. *1. Fe Catalyst Models.* Scheme 4 and Table 2 show the relative reaction Gibbs free energies and reaction pathways for Fe complexes. L′Fe first binds CO_2 to form L′Fe(CO_2) with a binding energy −9.3 kcal/mol, and L′Fe(CO_2) then goes through an endergonic reaction to form L′Fe(CO)(O) via transition state **Fe-TS-1** with a reaction barrier of 24.1 kcal/mol (steps B and C, ΔG_r (B + C) = 20.1 kcal/mol). Then L′Fe(CO)(O) experiences an endergonic dissociation reaction (step D, ΔG_r = 4.6 kcal/mol) and forms L′Fe(O), which then has a endergonic reaction with H_2 to generate L′Fe(OH) and H radical through a transition state **Fe-TS-2**, with a reaction barrier of 21.1 kcal/mol (steps E and F, ΔG_r (E + F)= 10.5 kcal/mol). In the following reaction, L′Fe(OH) and H form L′Fe(OH_2) (step G, ΔG_r = −18.2 kcal/mol),

Table 2. Reaction Gibbs Free Energies (ΔG_r, kcal/mol) Calculated Using B3LYP/aug-cc-pVTZ

	pathway									
metal	A	B	C	D	E	F	G(J)	H(K)	I(L)	$\Delta H^{\ddagger eff}$
Fe	−9.3	24.1	−3.2	4.6	21.1	−10.6	−18.2	10.7	−20.5	46.5
Mn	−9.0	36.5	−7.6	−5.4	15.1	−3.7	−10.9	17.2	−40.7	38.6
Co	−1.0	33.0	−4.6	3.1	19.1	−10.6	−23.7	12.1	−18.4	50.6

metal	M	N	O	P	Q	R	S
Fe	−58.9	36.5	−8.4	−71.9	−7.4	−27.0	−12.1

which then may go through a small barrier (step H, 10.7 kcal/mol) and rearrange to L′Fe(OH)(H). L′Fe(OH_2) can also release a H_2O molecule and form the catalyst again (discussed in ref 1).

On the other hand, it is easy to see that all diiron complexes have much lower energies than the mono-Fe systems: formation of L′Fe(CO)OFeL′ is highly exergonic (step M, ΔG_r = −58.9 kcal/mol), while cleavage of L′Fe(CO)OFeL′ to afford L′Fe(O) and L′Fe(CO) is very endergonic (step N, ΔG_r = 36.5 kcal/mol), indicating that formation of L′Fe(CO)OFeL′ is a thermodynamic sink and so dissociation to form L′Fe(O) and L′Fe(CO) is then difficult. Thus, it is more likely favorable for a catalytic process if L′Fe(CO)(O) dissociates into CO and L′Fe(O) directly, rather than reacting with another equivalent of L′Fe to form a diiron complex and then splitting into L′Fe(CO) and L′Fe(O). However, $(L'Fe)_2O$ can be formed by reaction of L′Fe(CO)OFeL′ and L′Fe (ΔG_r = −8.4 kcal/mol, step O) or by reaction of L′Fe(O) and L′Fe (ΔG_r = −71.9 kcal/mol, step P). Subsequently, L′Fe(CO_3)FeL′ may be generated by an exergonic reaction of $(L'Fe)_2O$ and CO_2 (step Q, ΔG_r = −7.4 kcal/mol), and then this carbonatediiron complex L′Fe(CO_3)FeL′ could dissociate into CO_3^{2-} and the original catalyst model L′Fe. The relative energies of L′Fe(CO)OFeL′, $(L'Fe)_2O$, and L′Fe(CO_3)FeL′ agree quite well with the previous research by Ariafard et al.[42] In the side reactions, additions of CO to L′Fe are strongly exergonic (step R, ΔG_r = −27.0 kcal/mol) as well as coordination of a second equivalent of CO to L′Fe(CO) (step S, ΔH_r = −12.1 kcal/mol).

In summary, from an energetic perspective, L′Fe(CO)(O) is very likely to react with an extra L′Fe and form a stable diiron complex L′Fe(CO)(O)FeL′, which will make ensuing catalytic steps difficult. The stability of diiron complexes $(L'Fe)_2O$ and L′Fe(CO_3)FeL′ is consistent with the experimental research by Holland et al.,[32,44] and the relative energies of L′Fe(CO)OFeL′, $L'Fe)_2O$, and L′Fe(CO_3)FeL′ are in good agreement with the research of Ariafard et al.[42] Obviously, bimetallic complexes engender thermodynamic sinks in the reaction coordinate and would thus retard RWGS catalysis. Thus, one important issue for realistic CO_2 catalysis by late metal complexes would require avoidance of dimetallic pathways and favoring monometallic pathways. For example, upon L′Fe(CO)(O) splitting into the reactive transient L′Fe(O) plus CO, the former could react with H_2 to favor the subsequent steps in RWGS catalysis. One may obviously attempt to inhibit formation of bimetallic complexes via the use of very bulky β-diketiminate substituents or sequestering complexes to a surface. Additionally, different metals may have different thermodynamic predilections for formation of bimetallic complexes. Hence, in order to explore the reactivity of

dx.doi.org/10.1021/ic200602v |*Inorg. Chem.* 2011, 50, 8782–8789

Scheme 5. Reaction Gibbs Free Energy Diagram for Mn Complex Reactions (B3LYP/aug-cc-pVTZ)

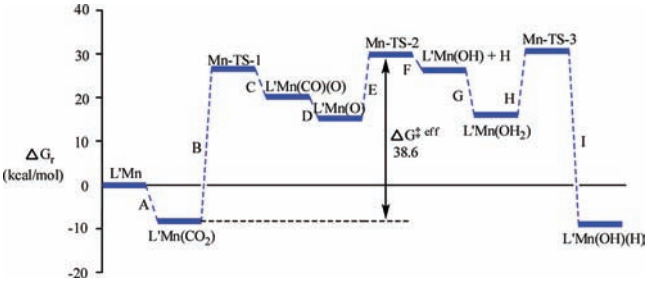

Scheme 6. Reaction Gibbs Free Energy Diagram for Co Complex Reactions (B3LYP/aug-cc-pVTZ)

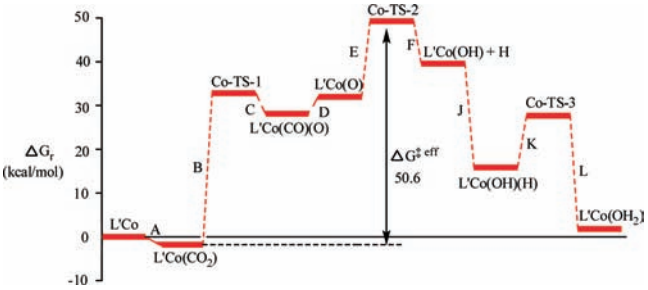

the catalyst models, we choose to compare and contrast catalytic pathways for Fe complexes as well as Mn and Co complexes.

2. Mn Catalyst Models. Many mono-Mn β-diketiminato complexes have been studied experimentally as well as some bimetallic versions.[26,51,52] For Mn complexes, the catalytic pathways display similar trends to the reactions of Fe complexes, where the monometallic reactions (steps A−I) delineate the preferred catalysis but bimetallic reactions (steps M−Q) generate unfavorable thermodynamic sinks. Generally, the energetic trend of Mn monometallic reactions is very similar to the trend of Fe reactions (Table 2 and Scheme 5), except that dissociation of CO from L′Mn(CO)(O) is exergonic (ΔG_r = −5.4 kcal/mol, step D) while for Fe it is endergonic (ΔG_r = 4.6 kcal/mol). Relative to Fe, bimetallic Mn complexes such as L′Mn(CO)OMnL′ tend to be "deeper" thermodynamic sinks, e.g., Mn has a calculated ΔG_r that is about 10 kcal/mol more exergonic for step M than Fe but 10 kcal/mol higher ΔG_r for step N, which forms L′M(CO_3)ML′ (see Supporting Information). Qualitatively, however, di-Mn reactions show the same thermodynamic trends as di-Fe reactions.

3. Co Catalysts Models. The results of the reaction Gibbs free energies and barriers show that Co complexes display similar energetics as compared to Fe and Mn complexes (Table 2 and Scheme 6). As expected, calculated thermodynamic data show that the final structure of the hydrogenation is more likely to be L′Co(OH_2), which has a slightly lower energy (3.9 kcal/mol lower) than L′Co(OH)(H). Dimetallic reactions were also calculated, as Fe and Mn reactions, to form a thermodynamic sink (see Supporting Information). However, compared to Fe and Mn, bimetallic Co complexes tend to be less exergonic in relation to monometallic complexes, e.g., formation of L′Co(CO)(O)CoL′ from the reaction of L′Co(CO)(O) and L′Co is less exergonic than that of Fe and Mn complexes (step M, ΔG_r (Co) = −57.5 kcal/mol, ΔG_r (Fe) = −58.9 kcal/mol, ΔG_r (Mn) = −69.2 kcal/mol) and the later step, splitting L′Co(CO)(O)CoL′ to L′Co(O) and L′Co(Co), is less endergonic than that of Fe and Mn complexes (step N, ΔG_r (Co) = 32.9 kcal/mol, ΔG_r (Fe) = 36.5 kcal/mol, ΔG_r (Mn) = 46.6 kcal/mol) (see Supporting Information). These results indicate that varying transition metal centers could steer the catalysis toward more favorable monometallic pathways.

d. Comparison of Different Transition Metals. In our previous research, which focused on the calculated thermodynamics of RWGS model component reactions, the middle members of the first-row transition metals were identified as the most promising catalysis. In this paper, therefore, the comparison is focused on the three middle transition series catalyst models, L′Fe, L′Mn, and L′Co. Assuming that ligand sets could be constructed to avoid/reduce formation of the bimetallics, this paper has focused on monometallic reactions. The kinetics of the whole catalysis process significantly depends on the effective reaction barrier, $\Delta G^{\ddagger}_{eff}$, the Gibbs free energy difference between the highest energy TS and the lowest energy point that precedes it. According to the mechanism we modeled, L′Mn shows the lowest $\Delta G^{\ddagger}_{eff}$ (38.6 kcal/mol, Table 2), implying the highest reaction rate. L′Fe has a higher calculated effective barrier (46.5 kcal/mol) than L′Mn, while a much higher $\Delta H^{\ddagger}_{eff}$ was calculated for L′Co complexes (50.6 kcal/mol).

Considering the individual reaction barriers, for activation of CO_2 (step B, Table 2), Fe shows the lowest barrier (23.9 kcal/mol) while Mn (38.1 kcal/mol) and Co (35.1 kcal/mol) have much higher barriers. For hydrogenation of L′M(O) (step E, Table 2), Mn has a slightly lower barrier (19.0 kcal/mol) than the other two metals (Fe 24.8 kcal/mol; Co 21.0 kcal/mol). In the rearrangement between L′M(OH_2) and L′M(OH)(H) (step H(K)), Fe also has a smaller barrier (11.6 kcal/mol) than Mn (15.8 kcal/mol) and Co (13.9 kcal/mol).

SUMMARY AND CONCLUSIONS

The catalytic cycle of a model reverse water−gas shift reaction using middle series 3d metal catalysts, L′M (M = Fe, Mn, and Co; L′ = parent β-diketiminate) has been investigated. The thermodynamics and reaction barriers of the elementary reaction pathways and side reactions were studied at two levels of theory: B3LYP/6-311+G(d) and B3LYP/aug-cc-pVTZ. All of the reactions were modeled in the gas phase at STP. Plausible catalytic mechanisms and a few side reactions were modeled, including formation of a set of monometal complexes (L′M(CO_2), L′M(CO)(O), L′M(O), L′M(OH), L′M(OH_2), L′M(OH)(H), L′M(CO), L′M($CO)_2$) and dimetal complexes (L′M(CO)OML′, (L′M)$_2$O, L′M(CO_3)ML′). According to the calculated thermodynamic and kinetic data, the most favorable catalytic cycle primarily involves monometallic complexes: the catalyst model L′M first reacts with CO_2 and forms a carbon dioxide complex L′M(CO_2), which then forms a carbonyl oxo complex, L′M(CO)(O); L′M(CO)(O) then releases CO and generates L′M(O), which reacts with H_2 to form either an aqua complex L′M(OH_2) (for Co) or a hydroxo hydride L′M(OH)(H) (for Fe and Mn). A transition state between the two tautomers, L′M(OH_2) and L′M(OH)(H), was also calculated.

The L′Mn model shows the smallest calculated fluctuation in calculated reaction Gibbs free energies. The complex L′Mn yields the lowest calculated effective reaction barrier, $\Delta G^{\ddagger}_{eff}$, calculated to be ∼8 kcal/mol lower than the calculated $\Delta G^{\ddagger}_{eff}$ for L′Fe. However, Fe also shows favorable kinetic properties, with the lowest barriers for the activation of CO_2 (breaking the C═O

dx.doi.org/10.1021/ic200602v |*Inorg. Chem.* 2011, 50, 8782–8789

bond) and for the conversion between L′M(OH_2) and L′M-(CO)(O). In summary, monometallic Mn β-diketiminato complexes provide the most desirable catalytic properties for the reverse water−gas shift reaction among the systems studied here.

In experiments, formation of bimetallic intermediates (e.g., from reaction of L′M(CO)(O) and L′M(O) with the catalyst L′M) would be a problem due to the great stability of the bimetallic complexes. Therefore, avoiding formation of such intermediates would be a challenge for this homogeneous catalysis. One direction to solve this problem is to modify the functional groups on the β-diketiminate ligand. For instance, substitution of hydrogen on the nitrogen and carbon atoms of the backbone with bulky groups would retard formation of bimetallics. Recently, several monometallic, monovalent complexes with β-diketiminate supporting ligation have been reported, for example, L^RNi(lutidine),[53] L^RCo(PPh_3),[54] and L^RFe(PPh_3).[28] Another direction would be to explore heterogeneous reactions. Metal centers play a significant role in catalysis;[8,13−16,55−58] thus, metal surface mediated scission of CO_2 is a possible strategy to avoid dimerization and oligomerization pathways to catalyst inactivation. On the other hand, according to the reaction Gibbs free energy diagrams of the monometallic reactions (Schemes 4−6), $\Delta G^{\ddagger}_{eff}$ depends on the energy difference between L′M(CO_2) and M-TS-2. Therefore, "pushing up" the energy of L′M(CO_2) by changing metal centers or perhaps using mixed metal complexes could reduce $\Delta G^{\ddagger}_{eff}$.

■ ASSOCIATED CONTENT

Supporting Information. Tables of total energies and Gibbs free energies of all complexes. This material is available free of charge via the Internet at http://pubs.acs.org.

■ AUTHOR INFORMATION

Corresponding Author
*E-mail: akwilson@unt.edu (A.K.W.).

■ ACKNOWLEDGMENT

The authors acknowledge the support of the United States Department of Energy (BER-08ER64603) and NSF CRIF (CHE-0741936) for equipment support.

■ REFERENCES

(1) Liu, C.; Munjanja, L.; Cundari, T. R.; Wilson, A. K. *J. Phys. Chem. A* **2010**, *114*, 6207.
(2) Walther, D.; Rubens, M.; Rau, S. *Coord. Chem. Rev.* **1999**, *182*, 67.
(3) He, L.; Wang, J.; Wang *J. Pure Appl. Chem.* **2009**, *81*, 2069.
(4) Sakaki, S.; Musashi, Y. *Inorg. Chem.* **1995**, *34*, 1914.
(5) Leitner, W. *Coord. Chem. Rev.* **1996**, *153*, 257.
(6) Costamagna, J.; Ferraudi, G.; Canales, J.; Vargas., J. *Coord. Chem. Rev.* **1996**, *148*, 221.
(7) Sakakura, T.; Choi, J. C.; Yasuda, H. *Chem. Rev.* **2007**, *107*, 2365.
(8) Baltrusaitis, J.; Grassian, V. H. *J. Phys. Chem. B* **2005**, *109*, 12227.
(9) Ohnishi, Y.; Matsunaga, T.; Nakao, Y.; Sato, H.; Sakaki, S. *J. Am. Chem. Soc.* **2005**, *127*, 4021.
(10) Darensbourg, D. J. *Chem. Rev.* **2007**, *107*, 2388.
(11) Isaacs, M.; Canales, J. C.; Aguirre, M. J.; Estiu, G.; Caruso, F.; Ferraudi, G.; Costamagna *J. Inorg. Chim. Acta* **2002**, *339*, 224.
(12) Li, J.; Jia, G.; Lin, Z. *Organometallics* **2008**, *27*, 3892.
(13) Liu, P.; Choi, Y. M.; Yang, Y.; White, M. G. *J. Phys. Chem. A* **2010**, *114*, 3888.
(14) Carter, E. A. *Science* **2008**, *321*, 800.
(15) Baltrusaitis, J.; Grassian, V. H. *J. Phys. Chem. B* **2005**, *109*, 12227.
(16) Li, S. F.; Guo, Z. X. *J. Phys. Chem. C* **2010**, *114*, 11456.
(17) Saha, D.; Bao, Z.; Jia, F.; Deng, S. *Environ. Sci. Technol.* **2010**, *44*, 1820.
(18) Arstad, B.; Fjellvåg, H.; Kongshaug, K. O.; Swang, O.; Blom, R. *Adsorption* **2008**, *14*, 755.
(19) Salles, F.; Ghoufi, A.; Maurin, G.; Bell, R. G.; Mellot-Draznieks, C.; Férey, G. *Angew. Chem. Int.* **2008**, *47*, 8487.
(20) Valenzano, L.; Civalleri, B.; Chavan, S.; Palomino, G. T.; Areán, C. O.; Bordiga, S. *J. Phys. Chem. C* **2010**, *114*, 11185.
(21) Lu, C. C.; Saouma, C. T.; Day, M. W.; Peters, J. C. *J. Am. Chem. Soc.* **2006**, *129*, 4.
(22) Chen, C.; Cheng, W.; Lin, S. *Catal. Lett.* **2000**, *68*, 45.
(23) Glezakou, V.; Dang, L. X. *J. Phys. Chem. C.* **2009**, *113*, 3691.
(24) Allen, O. R.; Dalgarno, S. J.; Field, L. D.; Jensen, P.; Turnbull, A. J.; Willis, A. C. *Organometallics* **2008**, *27*, 2092.
(25) Rankin, M. A.; Cummins, C. C. *J. Am. Chem. Soc.* **2010**, *132*, 10021.
(26) Bourget-Merle, L.; Lappert, M. F.; Severn, J. R. *Chem. Rev.* **2002**, *102*, 3031.
(27) Smith, J. M.; Lachicotte, R. J.; Pittard, K. A.; Cundari, T. R.; Lukat-Rodgers, G.; Rodgers, K. R.; Holland, P. L. *J. Am. Chem. Soc.* **2001**, *123*, 9222.
(28) Smith, J. M.; Sadique, A. R.; Cundari, T. R.; Rodgers, K. R.; Lukat-Rodgers, G.; Lachicotte, R. J.; Flaschenriem, C. J.; Vela, J.; Holland, P. L. *J. Am. Chem. Soc.* **2006**, *128*, 756.
(29) Ding, K.; Pierpont, A. W.; Brennessel, W. W.; Lukat-Rodgers, G.; Rodgers, K. R.; Cundari, T. R.; Bill, E.; Holland, P. L. *J. Am. Chem. Soc.* **2009**, *131*, 9471.
(30) (a) Pfirrmann, S.; Yao, S.; Ziemer, B.; Stösser, R.; Driess, M.; Limberg, C. *Organometallics* **2009**, *28*, 6855. (b) Pfirrmann, S.; Limberg, C.; Herwig, C.; Stösser, R.; Ziemer, B. *Angew. Chem.* **2009**, *121*, 3407. (c) Pfirrmann, S.; Limberg, C.; Herwig, C.; Stösser, R.; Ziemer, B. *Angew. Chem., Int. Ed.* **2009**, *48*, 3357.
(31) Pierpont, A. W.; Cundari, T. R. *Inorg. Chem.* **2010**, *49*, 2038.
(32) Sadique, A. R.; Brennessel, W. W.; Holland, P. L. *Inorg. Chem.* **2008**, *47*, 784.
(33) Holland, P. L. *Can. J. Chem.* **2005**, *83*, 296.
(34) Rose, R. P.; Jones, C.; Schulten, C.; Aldridge, S.; Stasch, A. *Chem.—Eur. J.* **2008**, *14*, 8477.
(35) Tsai, Y. C.; Wang, P. Y.; Lin, K. M.; Chen, S. A.; Chen, J. M. *Chem. Commun.* **2008**, 205.
(36) Monillas, W. H.; Yap, G. P. A.; Theopold, K. H. *Angew. Chem.* **2007**, *119*, 6812.
(37) Wang, Y.; Quillian, B.; Wei, P.; Wang, H.; Yang, X. J.; Xie, Y.; King, R. B.; Schleyer, P.; Schaefer, H. F., III; Robinson, G. H. *J. Am. Chem. Soc.* **2005**, *127*, 11944.
(38) Chai, J.; Zhu, H.; Stückl, A. C.; Roesky, H. W.; Magull, J.; Bencini, A.; Caneschi, A.; Gatteschi, D. *J. Am. Chem. Soc.* **2005**, *127*, 9201.
(39) Bai, G.; Wei, P.; Stephan, D. W. *Organometallics* **2005**, *24*, 5901.
(40) Dai, X.; Kapoor, P.; Warren, T. H. *J. Am. Chem. Soc.* **2004**, *126*, 4798.
(41) Dai, X.; Warren, T. H. *J. Am. Chem. Soc.* **2004**, *126*, 10085.
(42) Ariafard, A.; Brookes, N. J.; Stranger, R.; Boyd., P. D.W.; Yates, B. F. *Inorg. Chem.* **2010**, *49*, 7773.
(43) Hayes, P. G.; Piers, W. E.; Lee, L. W. M.; Knight, L. K.; Parvez, M.; Elsegood, M. R. J.; Clegg, W. *Organometallics* **2001**, *20*, 2533.
(44) Eckert, N. A.; Stoian, S.; Smith, J. M.; Bominaar, E. L.; Münck, E.; Holland, P. L. *J. Am. Chem. Soc.* **2005**, *127*, 9344.
(45) Frisch, M. J. et al. *Gaussian 09*, Revision A.02; Gaussian: Wallingford, CT, 2009.
(46) (a) Becke, A. D. *J. Chem. Phys.* **1993**, *98*, 5648. (b) Lee, C.; Yang, W.; Parr, R. G. *Phys. Rev. B* **1988**, *37*, 785. (c) Vosko, S. H.; Wilk, L.; Nusair, M. *Can. J. Phys.* **1980**, *58*, 1200. (d) Stephens, P. J.; Devlin, F. J.; Chabalowski, C. F.; Frisch, M. J. *J. Phys. Chem.* **1994**, *98*, 11623.
(47) Grimme, S. *J. Comput. Chem.* **2006**, *27*, 1787.
(48) All schemes are generated by Chemcraft (Version 1.6). http://www.chemcraftprog.com.

(49) Harvey, N. J.; Poli, R.; Smith, K. M. *Coord. Chem. Rev.* **2003**, *238*, 347.
(50) Poli, R.; Harvey, J. N. *Chem. Soc. Rev.* **2003**, *32*, 1.
(51) Chai, J.; Zhu, H.; Most, K.; Roesky, H. W.; Vidovic, D.; Schmidt, H.-G.; Noltemeyer, M. *Eur. J. Inorg. Chem.* **2003**, 4332.
(52) Chai, J.; Zhu, H.; Roesky, H. W.; He, C.; Schmidt, H.-G.; Noltemeyer, M. *Organometallics* **2004**, *23*, 3284.
(53) Wiese, S.; Kapoor, P.; Williams, K. D.; Warren, T. H. *J. Am. Chem. Soc.* **2009**, *131*, 18105.
(54) Dugan, T. R.; Sun, X.; Rybak-Akimova, E. V.; Olatunji-Ojo, O.; Cundari, T. R.; Holland, P. L. *J. Am. Chem. Soc.*, Articles ASAP. DOI: 10.1021/ja2052914.
(55) Glezakou, V.-A.; Dang, L. X.; McGrail, B. P. *J. Phys. Chem. C* **2009**, *113*, 3691.
(56) Allen, O. R.; Dalgarno, S. J.; Field, L. D. *Organometallics* **2008**, *27*, 3328.
(57) Wang, G.; Nakamura, J. *J. Phys. Chem. Lett.* **2010**, *1*, 3053.
(58) Peña O'Shea, A. V.; González, S.; Illas, F.; Fierro, L. G. J. *Chem. Phys. Lett.* **2008**, *454*, 262.